

# Magneto-optic Response of Iron Oxide Nanoparticles under Pulsed and AC Fields

T. Foulkes\*, M. Syed\*\* and B. Kodalen\*\*

Electrical Engineering\* and Physics\*\* & Optical Engineering Department  
Rose-Hulman Institute of Technology  
5500 Wabash Ave., Terre Haute, IN 47803

## ABSTRACT

Reliable methods for studying the magnetization dynamics of metal ferrite nanoparticles (NP) are needed, as these particles are attractive candidates for biomedical applications such as in targeted drug delivery, molecular imaging, and magnetic hyperthermia [1-2]. In this study, magnetic response of various iron oxide NP in aqueous solution was investigated by performing Faraday Rotation (FR) experiments under pulsed fields (typically 0.6 Tesla and 100 to 300 ms in duration) and as a function of excitation frequency using the magneto-optic technique of AC Faraday rotation. Comparisons of the results yield interesting insights about the behavior of these particles in different field environments. This comparative analysis also suggests how AC and Pulsed measurements can yield complimentary information that can provide a more detailed understanding of the magnetization process in these systems.

**Keywords:** Néel Relaxation, Brownian Relaxation, Faraday rotation, Pulsed Magnetic Fields

## 1 INTRODUCTION

Solutions of varying concentration were prepared from  $\text{Fe}_3\text{O}_4$  (Magnetite) and  $\text{Fe}_2\text{O}_3$  (Maghemite) NPs having an average diameter of 10 nm. For the AC technique, over the range of magnetic field frequencies studied, the magnitude of the Faraday rotation (FR) of these solutions was found to decrease nonlinearly with increasing frequency. The magnetization of the solutions, being proportional to the FR, follows the same trend. The AC measurement technique can detect differences in rotation less than a tenth of an arc minute in magnitude, and is sensitive to changes in the solutions' NP volume fractions as small as  $2 \times 10^{-6}$ . On the other hand, strength of the pulsed field method lies in the fact that it can provide a live "snapshot" of the magnetization dynamics [3]. Especially noteworthy is the presence of the relaxation plateaus that can be related to Néel and Brownian relaxation modes that are typical of NP response in magnetic fields. Pulsed magnetic fields can represent a direct measurement approach for finding out these vital parameters for NP systems. Our pulsed field results also show a weak ferromagnetic phase for NP concentrations usually determined as super paramagnetic.

While the largest particles in the AC method cease to participate in the magnetization as their relaxation time becomes longer than the switching time of the field, they

still contribute to the relaxation plateaus that characterize the NP response under magnetic field pulses. This two-prong analysis of magnetization dynamics will complement future work which seeks to understand the effects of nanoparticle bonding with bio molecules and the resulting changes to the particles' hydrodynamic radii and relaxation times.

## 2 BACKGROUND

### 2.1 Physical Principles Behind FR

Simply, FR is a useful magneto-optic technique to investigate the magnetic properties of both homogenous solid and liquid samples and nonhomogeneous samples such as complex liquid systems or colloids composed of solid nanoparticles dispersed in a liquid. Also known as the Faraday effect, FR refers to magnetically induced birefringence whereby the electric field polarization vector of a light beam rotates as it passes through a sample in the presence of a magnetic field [4]. When Michael Faraday reported his observations regarding this phenomenon in 1854, he established a fundamental relationship between magnetism and light and provided early evidence for the underlying electromagnetic structure of all elements and compounds, which has helped to develop modern theories of atomic structure and the electromagnetic wave nature of light [5]. Physically, since the index of refraction is no longer in the same direction, this magnetically induced birefringence or anisotropy highlights how light with different polarization orientations propagates at different speeds through a material [6]. Consequently, as the electric field vector  $E$  of the linearly polarized light from a laser

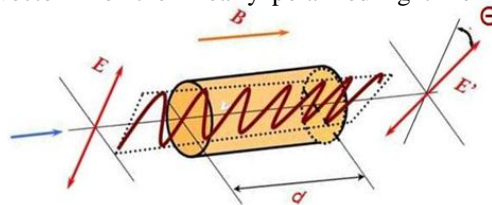


Figure 1: Rotation of polarized light during FR

passes through a medium of length  $d$  inside a magnetic field with a magnetic flux density of magnitude  $B$ , this polarization orientation rotates an angle  $\theta$  as depicted in Fig. 1 [7]. Summarized in (1), this rotation is the product of the magnitude of the magnetic flux density, the length of the sample or optical path length,  $d$ , and the Verdet constant,  $V$ . For AC Faraday Rotation, units for this equation are:  $\theta$  [arcminutes],  $V$  [arcminutes/G\*cm],  $B$  [G],

and  $d$  [cm]. For Pulsed Faraday Rotation, units for this equation are:  $\theta$  [degrees],  $V$  [degrees/tesla-cm],  $B$  [tesla], and  $d$ [cm]. As a reference, 1 degree = 60 arcminutes and 1 tesla =  $10^4$  gauss.

$$\theta = B \cdot d \cdot V \quad (1)$$

## 2.2 Significance of the Verdet Constant

Every material has a unique Verdet constant that characterizes its magnetic properties. The Verdet constant typically exhibits dispersion (wavelength dependence). Verdet constant can help deduce a material's magnetization and dependence of magnetization on various material and environmental parameters of interest (e.g., NP shapes, concentration, sample temperature, etc.).

## 2.3 Longitudinal Polarization Orientation

For this study, the traditional longitudinal measurement was employed since it yields information regarding first order effects of magnetic response for materials. For this polarization orientation, the plane containing the electric field vector of the linearly polarized light is always perpendicular to the magnetic flux density vector in the longitudinal FR measurement.

# 3 EXPERIMENT

## 3.1 AC & Pulsed Experimental Setups

As depicted in Fig. 2, a basic Faraday rotation experimental setup involves: a linearly polarized light source, a source of external magnetic field, a secondary polarizer, in the blue circle, referred to as the analyzer, and a photo detector, (photodiode from Thorlabs, DET 110). While a HeNe laser (1.5 mW JDS Uniphase) provides linearly polarized light at a wavelength of 633nm, a primary polarizer should be inserted in the optical path to control the intensity of light entering the sample in order to reduce the local heating of the sample. Next, an analyzer is oriented at 45 degrees with respect to the first polarizer in order to maximize the response of the setup [8]. In-between these two polarizers, the beam passes through the sample that is placed at the center of a long solenoid, which has been designed to provide uniform internal magnetic field in order to simplify the process determining the magnitude of the magnetic flux density through the sample.

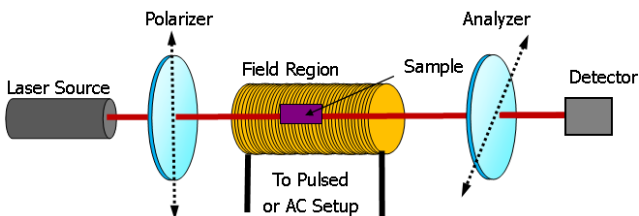


Figure 2: Important aspects of a FR experimental setup

This setup is very robust because either pulsed and AC magnetic fields can be generated based on the excitation circuit connected to a solenoid. For the AC setup, a sinusoidal signal from a function generator excited an RLC circuit containing the solenoid (1.3 mH, 710 turns, 2.0 inch dia.) after enlarging the signal with a 120-watt power amplifier. In order to examine the magnetic response of NPs at various frequencies, the experiment was repeated for five distinct capacitance and resonant frequency settings. The need for impedance mismatch corrections between the AC and the DC signals was overcome by measuring both the RMS amplitude of the AC component and the DC background component of the signal at different times throughout the measurement process using a lock-in amplifier (Model SR830 DSP), which received its reference from the function generator. Since the analyzer was always set at 45 degrees with respect to the first polarizer in order to maximize the response of the setup, the ratio of the AC amplitude and the DC component determined the amplitude of the rotation based on the method summarized by Alope, et al [9]. After plotting the amplitude of the rotation for several values of magnetic field strength, the slope of a best fit revealed the Verdet constant.

The block diagram of a pulsed magnetic field circuit depicted in Fig. 3 contains five essential circuit elements: a power supply, safety circuit elements, a capacitor bank as an energy storage mechanism, an IGBT as a precision switch, and an inductive load such as a solenoid for creating the external magnetic field for the Faraday rotation experiment. More details regarding the rationale for this design have been discussed elsewhere [10].

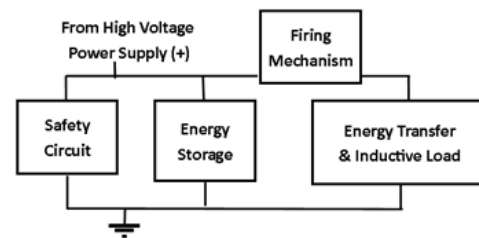


Figure 3: Block diagram of pulsed magnetic field circuit

Probing the Faraday effect of a system using a pulsed magnetic field has many advantages over the AC setup. To begin with, a solenoid was designed (self-inductance of 6.5 mH, 610 turns, and ESR of 5.17 ohms) to generate an applied current pulse with a peak current magnitude of 200 amperes, a pulse duration of 300 milliseconds, and a peak rise time of 8 milliseconds for maximum capacitor charging voltage of 400 V. Simply, the peak magnitude of the magnetic flux density generated for this setup is approximately 0.6 Tesla or 6,000 Gauss, which is approximately 100 times larger than that of the AC setup. As a result, the maximum induced angle of rotation for the longitudinal Faraday effect has been on the order of 1 to 3 degrees, which is significantly greater than the rotations recorded for the AC setup in fractions of arcminutes. Before

implementing both FR setups, the analyzer is rotated with no field applied to check for any optical activity and is then returned to the 45 degree starting orientation.

### 3.2 Interpreting Pulsed Measurements

As depicted in Fig. 4, the combination of the analyzer's setting and the direction of the polarization vector's rotation in the material results in a change in the light intensity incident on the photo detector. If the electric field polarization vector rotates toward a parallel alignment with the analyzer's polarization axis (a), then the light intensity incident on the photo detector increases and the output voltage increases. In contrast, an induced rotation, (b), causing this alignment to be more orthogonal will decrease the intensity of the light incident on the photo detector, which will decrease the detector's output voltage. Finally, when no external magnetic flux density is applied, this is the reference case for all AC and pulsed setup measurements. Measurements are taken for both analyzer settings (a) and (b) in order to verify the results since for pure liquid systems such as water and for solids are equal and opposite.

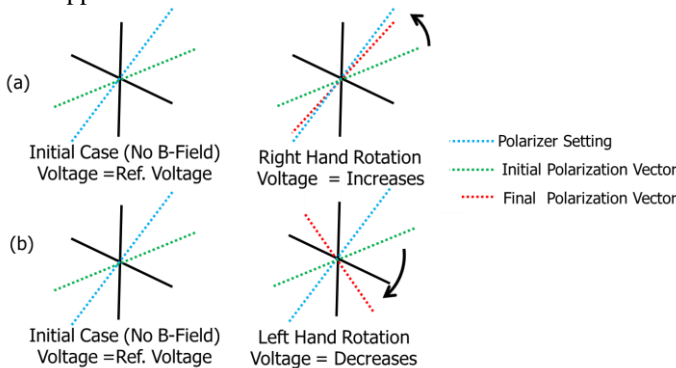


Figure 4: Correlating rotation to changes in intensity

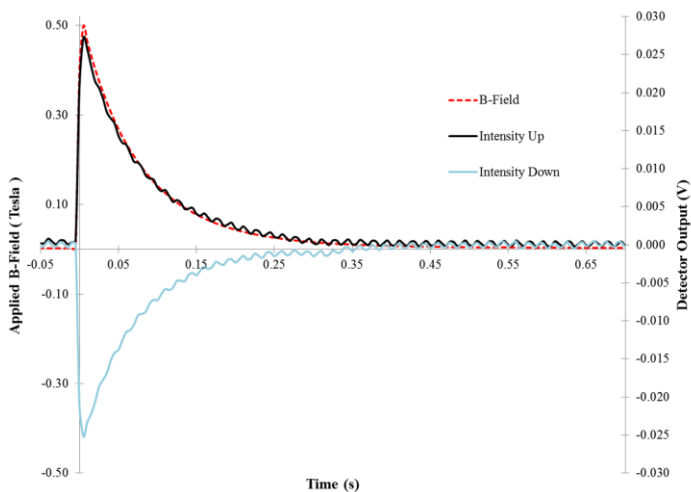


Figure 5: Understanding the rotation direction with intensity profile for "up" and "down" water pulses

As depicted in Fig.5 with results from measuring water with pulsed FR, if the output of the detector for a given rotation with an analyzer setting (a) is 25 millivolts "up" from the reference, then the output of the detector for a given rotation of the same conditions with an analyzer setting (b) will be 25 millivolts "down" from the reference. Due to this characteristic deviation from the reference, the labels of "up" and "down" have been chosen to classify the (a) and (b) analyzer settings respectively and help determine the handedness of rotation. In Fig. 5, the dashed red line corresponds to the profile of the current pulse and thus represents the magnetic flux density pulse.

### 3.3 Nanoparticles Investigated

For this investigation, three different types of NPs were examined. The first referred to as EG441 were bare  $Fe_2O_3$  NPs with diameters of 10.0 nm as verified by TEM. They are in a water solution with a pH of approximately 2. The sample solution is 0.2M in iron (16 g/L in Maghemite). Measurements were carried out on samples that were diluted from the the stock solutions with high-purity water (resistivity 18.0 M $\Omega$ /cm). Room temperature magnetization curves show paramagnetic behavior (no hysteresis) and the saturation magnetization for samples EG441 was measured to be 62.4 emu/g. The second type of NP was the commercially available  $Fe_3O_4$  with a nominal size of 10nm and a size distribution ranging from 5-15 nm. For EMG807 five varying concentrations from 10uL to 30uL were added to 10mL of the ultra-pure high resistivity water. Preparation and other details of these samples have been discussed elsewhere [11-12].

## 4 RESULTS & FUTURE WORK

As depicted in Fig. 6, the Verdet constant for each concentration of EMG807 decreases linearly on this log scale as the excitation frequency of the AC FR measurement increases, which is in sharp contrast to the generally constant value for the Verdet constant of water. The noticeable decrease in water's Verdet constant at 10kHz is a significant factor in the large, uniform decrease of all EMG807 Verdet constant at 10kHz. Yet, this result from the AC FR technique can only provide static, time-averaged information about the magnetic response of a system for a small spectrum of magnetic fields well below saturation magnetization. In contrast, Fig. 7 highlights how the pulsed FR technique can highlight the dynamic features of the an MNP's magnetic response such as the formation of distinct relaxation slopes and the presence of multiple relaxation regimes. The fast response of the system is related to the Néel magnetic response mode, which involves the fast realignment of magnetic dipoles in orientation with the external magnetic field, while the long relaxation response is related to the physical relaxation of the particles due to Brownian motion, the slow magnetic response mode.

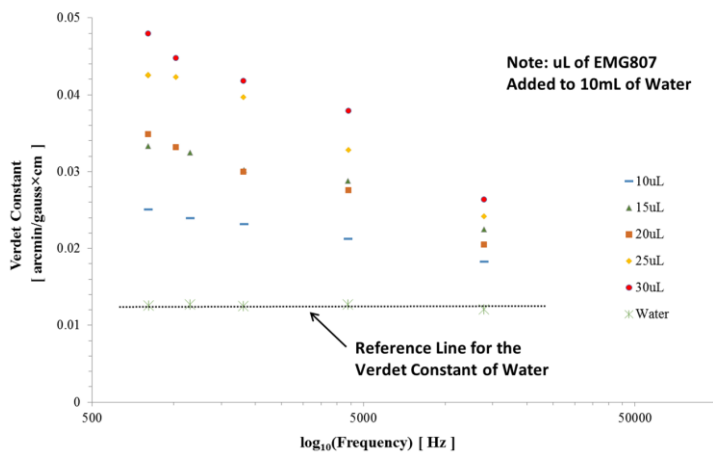


Figure 6: Impact of frequency on the Verdet Constant of EMG807 for varying concentrations

Additionally, as concentration of MNPs increases, the peak magnetic response increases, but the intensity signal profile still crosses the reference at ~0.5 seconds before returning to the self-referencing value. This self-referencing feature highlights the robust nature of the pulse measurement. This crossing of the reference line is indicative of the opposite rotation to that of water by the EMG807 NPs.

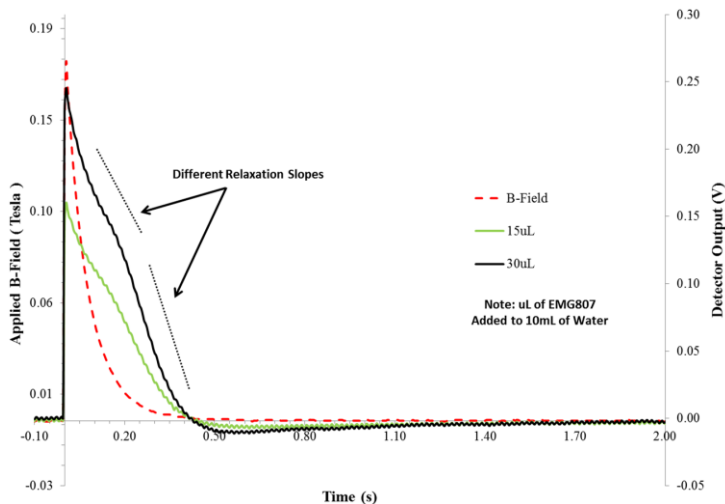


Figure 7: Intensity signal profile for EMG807 and the impact of concentration on characteristics of relaxation

Moreover, Fig. 8 highlights how the EG441 NP's magnetization persists for more than two seconds after the influence of the external magnetic field ends at 0.3 seconds. These results are exciting because they deviate significantly from the dynamic magnetic response of deionized water, depicted in Fig. 5, which is in strong agreement with the shape of the magnetic flux density pulse. This result contains both Néel and Brownian motion relaxation.

As part of future work, our forthcoming paper will discuss how these distinct slopes are either from aggregation effects or from the size distribution of the nanoparticles. Also, results from direct but more expensive

techniques such as TEM, for particle counting and for characterizing particle size distribution will be compared in order to highlight the potential of these relatively straightforward and inexpensive optical techniques to perform these tasks.

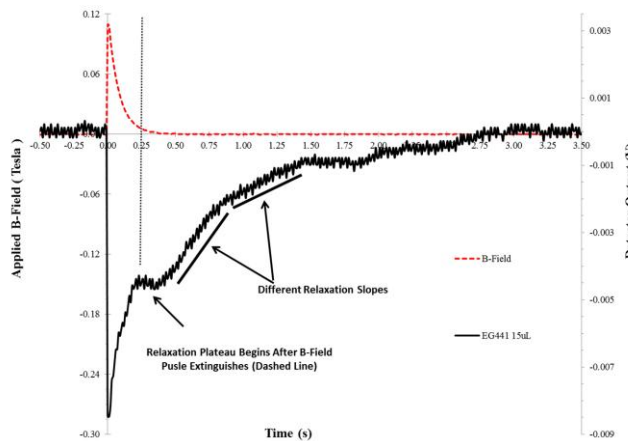


Figure 8: Intensity signal profiles: EG441(a), EG442(b)

## REFERENCES

- [1] M. Arruebo, R. F. Pacheco, M. R. Ibarra, and J. Santamaría, *Nano Today* 2, 22-32 (2007).
- [2] R. Hergt, et al., *J. Magn. Magn. Mat.* 270, 345-357 (2004).
- [3] Helen W Davies and J Patrick Llewellyn, "Magnetic birefringence of ferrofluids. II. Pulsed field measurements," *J. Phys. D: Appl. Phys.*, vol. 12, pp. 1357-63, 1979.
- [4] P.C. Scholten, "First Century of Colloid Magneto-Optics," *Indian Journal of Engineering and Material Sciences*, vol. 11, pp. 323-330, Aug. 2004.
- [5] Sir C.V. Raman, F.R.S., "India's Debt to Faraday," *Nature*, vol. 128, pp. 362-364, 1931.
- [6] Judith F. Donnelly and Nicholas M. Massa, *Light: Introduction to Optics and Photonics*. New England Board of Higher Education, 2007
- [7] Matesy GmbH, Schematic graph of the Faraday rotation.
- [8] A. Jain, J. Kumar, F. Zhou, L. Li, and S. Tripathy, *Am. J. Phys.* 67, 714-717 (1999).
- [9] A. Jain, J. Kumar, F. Zhou, L. Li, and S. Tripathy, *Am. J. Phys.* 67, 714-717 (1999)
- [10] Thomas Foulkes, Dr. Maarij Syed, and Dr. Marc Herniter, *IEEE 56<sup>th</sup> International Midwest Symposium on Circuits and Systems*, Columbus, Ohio, 2013, pp. 497-500.
- [11] C. de Montferrand, et al., *Acta Biomaterialia*, 9 (4), 6150-6157 (2013).
- [12] <https://ferrofluid.ferrotec.com/ferrofluid-home>